VOL. 10, NO. 4, MARCH 2015 ISSN 1819-6608
ARPN Journal of Engineering and Applied Sciences


www.arpnjournals.com

GA BASED OPTIMIZATION OF THE PRELIMINARY DESIGN OF AN EXTREMELY HIGH PRESSURE CENTRIFUGAL COMPRESSOR FOR A SMALL COMMON RAIL DIESEL ENGINE

Luca Piancastelli and Leonardo Frizziero
Department of Industrial Engineering, Alma Mater Studiorum University of Bologna, viale Risorgimento, Bologna, Italy
E-Mail: leonardo.frizziero@unibo.it

ABSTRACT

A method to perform the preliminary design of an impeller for an extremely high pressure ratio centrifugal compressor is introduced in this paper. The equations used are fully detailed and a design procedure is introduced. This design procedure required a GA (Genetic Algorithm) optimization to obtain an acceptable optimum result. It is demonstrated that a 8:1 compressor can be designed for a mass flow of 500 kg/h. This GA optimized initial design should be then be validated through CFD (Computational Fluid Dynamics) simulation and then tested on a test bench. However, the initial design phase is critical, since a CAD model of the impeller is needed to start the simulation process. In our case this initial phase couldn't be inspired by existing design, since none were found. Aircraft and Helicopter engines do not have the problem of turbo lag, since fan/propeller inertia eliminates this problem. On the contrary these engines necessitate of performance at altitudes (flight levels) much higher than automotive applications. Small turbochargers with high compressor ratio are not available on the market, so a special design is needed.

Keywords: centrifugal compressor, GA, rail diesel engine.

INTRODUCTION

The research of aircraft engines moves towards increasing power to weight ratio, with reduced fuel consumption and with the restore altitude higher possible. Thanks to the innovations made in recent years in the Direct Injection Diesel (DID) engines, the power to weight ratio of these engines has been greatly increased. This fact, together with their very good efficiency has led to a great interest for aircraft and helicopter applications.

At an altitude of 20,000ft (6,100m) in the International Standard Atmosphere (ISA) the density of air is reduced to half of what it is at sea level. . Without working on the turbo charging, a DID loses 50% of its sea level power when at 20,000ft.An aircraft in climb would experience a lower mass of air entering the cylinders; the result is a decrease in the output power of aircraft engine In DIDs, this problem may conduct the engine to a full stop without the possibility of hot restarting.

For all the above factors, but particularly to enable a higher restoring altitude, it was decided to study a single stage, extremely high ratio, turbo charging system. A very small turbocharger was preliminarily designed; since small high-ratio compressors are very difficult do design with acceptable efficiency.

In this context the project of the conversion of the Direct Injection Diesel (DID) FIAT 1.9 Jtd 8V (8 Valves) is a very interesting. In single turbocharger systems, the induction system is composed by the air intake, the air filter, the compressor ant the after cooler. As altitude reduces the air density it is possible to recover it by increasing boost pressure. This is normally achieved by increasing the turbocharger rotational speed. The altitude at which the nominal boost pressure can be maintained is called recovery altitude. Up this Flight Level (FL) the engine will output its original output power with a small increase of Specific Fuel Consumption (SFC) due to the increased compression work. From the recovery altitude up the DID engine will not only lose power. It will also lose the possibility of starting (not only cold starting, but also hot restarting) and the possibility of full throttle authority. So for modern turbocharged common rail DIDs five altitudes are significant. Recovery altitude (1) that is the altitude at which the engine maintains nominal full power and full throttle authority. Starting altitude (2) that is the altitude at which the engine can be started-up (hot starting). Full throttle authority altitude (3), that is the altitude at which the throttle can be freely used. From this altitude up the throttle must be kept to "continuous full". The engine will continue to run with an output power that decreases with altitude. Maximum altitude (4), that is the altitude at which the engine will continue to run (ignite). These four altitudes are meant for ISA (ISA+0°C) conditions. Offsets from this conditions define different altitudes. A common temperature envelope is (ISA-50°C)-(ISA+20°C). This means (-35°C)-(+35°C) at sea level. So an engine will have 3 sets of 4 altitudes, a set for the minimum temperature (for example ISA-50°C), a set for nominal conditions (ISA+0°C) and a set for maximum temperature (ISA+20°C). The performance (power and torque vs rpm) will be matched with the 3rd direction (the altitude). Unfortunately, especially for low power levels, the automotive turbochargers are optimized for low inertia, high torque at low rpm and reduced turbolag. All these factors unavoidably took the designer to multistage/parallel multiunit systems even for compression ratios below 4:1.

In aircrafts and helicopters, the turbolag problem is annihilated by the high inertia of propellers and fans. Extremely high compression ratio turbochargers are necessary even for small displacements and power

outputs. This units should be very efficient, but do not need the brilliant dynamic of automotive turbo charging, since the normal operational field is from 50% to 100% rpm and output power for aircrafts. For helicopters it is from 98% to 100% rpm with loads from 75% to 100%. For this reason a very special turbocharger unit was developed for a well known engine (FIAT 1900jtd 8 valves) with the aim to reach the maximum compression ratio possible.

The design goal is to build a centrifugal compressor with the following key features: extremely high compression ratio; simplified form that allows to build the prototype and to avoid tricking problems in the final set-up, the possibility to use a set of commercial journal bearings. In order to achieve the maximum compression ratio possible, it was chosen to use a straight vaned compressor. So in the impeller the vanes are perfectly radial (in this way also the mechanical resistance to the centrifugal force is increased). The inducer is arc shaped and the channel passage does not comply In practice our compressor gives up a good fluid dynamic efficiency in exchange for the high compression ratio that is intended to achieve. To perform the sizing calculations of the impeller, we used set of formulas. As can be seen from Figure-1, the prototype of the impeller is schematized into three distinct elements (suitably connected together): the vane/blade (the wheel), the disk and the hub sections.

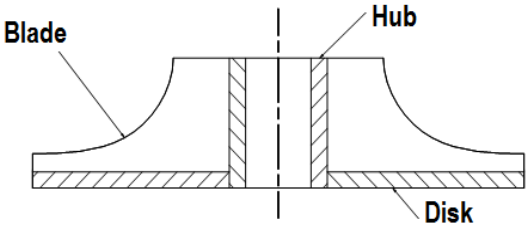

Figure-1. the impeller.

A front view (Figure-2) of the impeller highlights the inducer that is known as having an axial flow and is designed to receive the incoming flow.

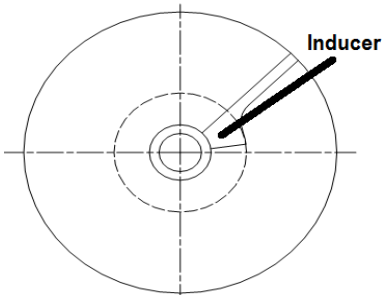

Figure-2. Frontal view of the impeller. Only a blade is depicted.

Figure-3 shows a representation of the triangles of the fluid velocity in the inlet section of the impeller (section 1) and in the output section (section2). As you can see from the picture the two velocity triangles belong to two different planes perpendicular to each other: it is easy to understand if you remember that the impeller forces the incoming flow that has come out in the axial direction to the radial direction.

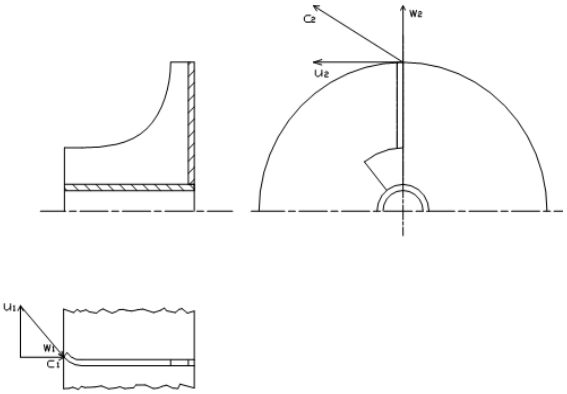

Figure-3. Conventions on velocity vectors.

Note that in Figure-3 is the inducer is represented in a simplified form with axial flow .It is necessary to make a few brief comments on the velocity triangles shown in Figure-3: C1 (the absolute velocity of the incoming stream) has a perfectly axial direction. The outflow has a perfectly radial relative velocity (the radial direction is W2) because it was chosen to have completely radial vanes. This output flow is based on the assumption that the vanes is perfectly able to guide and therefore the relative velocity vector has a direction perfectly coincident with the tangent to the vane in the trailing edge (diversion). This hypothesis cannot be considered valid for compressors because it would lead to unrealistic results, even a certain unevenness of the flow (due to the phenomenon of separation).

Actual flow output from the impeller

This procedure to correct the W2 was proposed by Traupel and allows us to study separately the two phenomena (diversion +non-uniformity). It is assumed that the deviation does not change in any way the radial components of the vectors, and leads to a change of the tangential components, of the absolute velocity and the relative velocity. It is, therefore, defined slip-factor as the ratio of the tangential components of the velocity and absolute. To calculate it we use the Wiesner formulation (1) (see Figure-4):

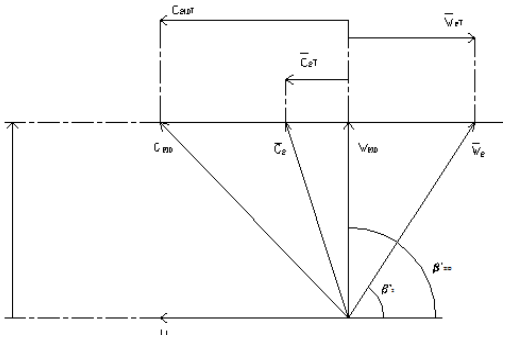

Figure-4. Deviation of output velocity.

$$\mu = 1 - \frac{\sqrt{sen\beta'_{2ID}}}{Z^{0,7}} \tag{1}$$

and then

$$C_{2IDR} = \overline{C}_{2R} = W_{2IDR} = \overline{W}_{2R}$$

$$COTG\beta'_2 = \mu COTG\beta_{2ID} + \frac{1-\mu}{\overline{C}_{2R}}$$

$$\overline{C}_{2T} = \mu C_{2IDT}$$

$$\overline{C}_2 = \sqrt{\overline{C}_{2R}^2 + \overline{C}_{2T}^2}$$

$$\overline{W}_2 = \frac{\overline{W}_{2R}}{sen\beta'_2} \tag{2}$$

We know now, so completely the velocity triangle that represents the diverted output flow is then known. From experimental findings it has been understood that the flow between two consecutive vanes presents an obvious unevenness due to a complex phenomenon of flow separation. The easiest way to take account of this phenomenon is that proposed by Dean and Senoo where it is assumed that the flow is composed of two distinct zones (Jet,Wake), characterized by different speeds, as seen from Figure-5:

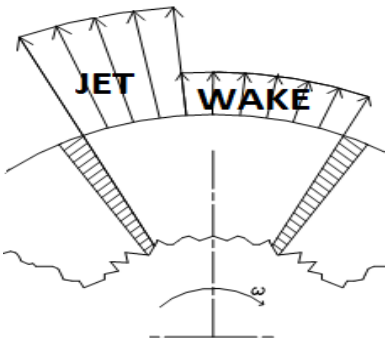

Figure-5. wake and jet zones.

The "wake" area relatively low speed output from the impeller forming a sort of obstruction to the passage of the flow; so it can therefore be assumed that only available area is the "jet" one. We start from the triangle of velocity of the diverted flow previously calculated (2) $\overline{C}_2; \overline{W}_2; U_2$. We make a further correction to take into account of the "wake and jet" phenomenon. It should be noted that we always work with average speed vectors. The result will be a new C_2,W_2,U_2 triangle. As seen from Fig.6 the triangle of the new actual speed is characterized by a speed that has the same direction (therefore remains equal to the angle), but a larger module. To be able to "pass" from the triangle to the triangle of velocities is calculated a coefficient of obstruction to the passage of the flow due to the WAKE area (3) (4).

$$\xi_W = \frac{\overline{C}_{2R}}{C_{2R}} = \frac{\overline{W}_{2R}}{W_{2R}} \tag{3}$$

$$\xi_w = 1 - (0{,}15 + 0{,}004\beta'_{2ID})(1 - \frac{\overline{W}_2}{W_1}) \tag{4}$$

We have from figure 6 that:

$$C_{2R} = W_{2R} \quad \text{and} \quad \overline{C}_{2R} = \overline{W}_{2R}$$

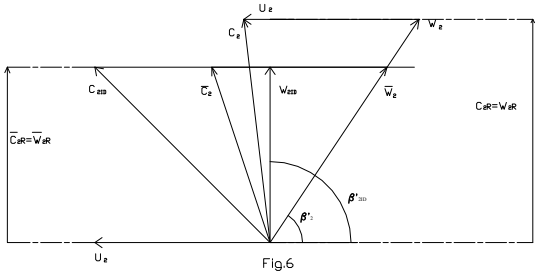

Figure-6. New triangles due to wake jet phenomenon.

It is then possible to calculate the new the triangle of speed $C_2; W_2; U_2$ using the following formulas (5):

$$W_{2R} = \frac{\overline{W}_{2R}}{\xi_W} = C_{2R}$$

$$W_2 = \frac{W_{2R}}{sen\beta'_2}$$

$$C_2 = \sqrt{W_2^2 + U_2^2 - 2W_2U_2\cos\beta'_2} \tag{5}$$

Calculation of the vane obstruction

In this one-dimensional model is assumed that the flow conditions in a generic section (speed, temperature, etc.) are constant and equal to those calculated at the point

of the section that belongs to the midline. The mass balance equation should hold:

$$\dot{m} = \rho A V \tag{6}$$

Initially, the area of passage is calculated in the hypothesis that there are no vanes (extremely thin vanes). The presence of the vanes is then taken into account with the correction coefficient ξ (coefficient of obstruction). We define, therefore, ξ in the following manner:

$$\xi = \frac{A_P}{A_{PID}} \tag{7}$$

Now the mass flow continuity equation (6) is applied in the sections of the input and the output of the impeller (Figure-7) (8) (9) (10):

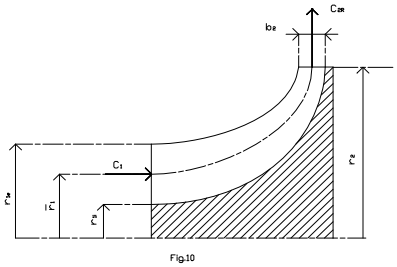

Figure-7. Input and output sections of the impeller.

$$\dot{m} = \rho_2 \cdot C_{2R} \cdot A_2 \tag{8}$$

$$A_2 = 2\pi r_2 \cdot b_2 \cdot \xi_2 \tag{9}$$

$$\dot{m} = \rho_1 \cdot C_1 \cdot A_1 \tag{10}$$

Relationship between compression ratio and the peripheral speed of the impeller

In the three previous paragraph we have defined a methodology that allows us to analyze the flow in the impeller. It is also necessary, however, to carry out a thermodynamic analysis in order to tie up the the variables of the design process. The initial data of our design are the inlet mass flow to the engine (500 kg/h) and the compression ratio that is the higher possible. An initial tentative value is 8:1. This is the starting point of the whole design. The higher is the compression ratio, the better the product The choice of this data is based on the possibility to build impellers with peripheral speeds exceeding 600 m / s with compression ratios higher than 8 ([1], chapter 6, pg. 473). The basic equation is the following [1][2] (11):

$$U_2 = \sqrt{\frac{k}{k-1} RT_A^0 \left\{ \frac{1}{\eta_C \Psi} \left[\left(\frac{P_B^0}{P_A^0} \right)^{\frac{K-1}{K}} - 1 \right] \right\}} \tag{11}$$

U2 is the pheriperal speed of the impeller, while ψ is the "coefficient of work". This is defined as follows:

$$\Psi = \frac{L}{U_2^2} \tag{12}$$

The specific work of L is defined as the specific work of the impeller with the true velocity vector, but with an adiabatic transformation (13) [1]:

$$\Psi = 1 - \frac{C_{2u}}{U_2} \cot g \beta_2 \tag{13}$$

Impeller thermodynamics

From (8) and (9) it is possible to obtain (14):

$$\dot{m} = \rho_2 \cdot C_{2R} \cdot 2\pi r_2 \cdot b_2 \cdot \xi_2 \tag{14}$$

If we suppose to set the values of ξ_2, b_2 being known $\dot{m}, C_{2R}$, the only variable that we have to determine is the density of the fluid in the output section ρ_2. This can be easily calculated (11) (12) (13):

$$P_2 = P_1 \left[1 + \frac{k-1}{2} \cdot \eta_G \cdot \frac{W_1^2 + \left(U_2^2 - U_1^2\right) - W_2^2}{kRT_1} \right]^{\frac{k}{k-1}} \tag{15}$$

$$T_2 = T_1 \left[1 + \frac{k-1}{2} \cdot \frac{W_1^2 + \left(U_2^2 - U_1^2\right) - W_2^2}{kRT_1} \right] \tag{16}$$

$$\rho_2 = \frac{P_2}{RT_2} \tag{17}$$

ρ_2 can be then calculated in this way. It value can be used in equation (8) to determine the diameter of the impeller $D_2 = 2r_2$.

Dimensionless approach to impeller design

In the four previous sections we have introduced the variables and formulas that will be useful for the design of the impeller. Our goal in this section is to explain the design method that was followed. For this purpose it is particularly convenient to use dimensionless velocity vectors. This is accomplished by dividing the speeds by U_2 (impeller peripheral speed). The advantage of this technique is that you can work with the

dimensionless velocity triangles to calculate the coefficient of work ψ and then equation (9) can be used to evaluate U_2.

Outer impeller diameter optimization

The calculation of the outer diameter of the impeller has been executed with the aid of the Genetic Algorithm (GA). In fact it is necessary to assume a set of initial values, within a reasonable range. When the design procedure is finished, the efficiency is estimated. This value should match with the initial assumption of the input. For this reason several input sets should be tested to obtain a reasonable impeller design. This process has been automated with the GA. To simplify the explanation of the procedure the "final optimized set of input values" found by the GA has been indicated directly in the explanatory input set. However several thousands of simulations have been carried out by the GA to find this optimum acceptable value. With the method introduced herein, it is necessary to assign tentative values to the following variables: Z=18, β'_{2ID} =(construction vane angle at the impeller outlet)=0,

$$\xi_2 = 0.955, \frac{b_2}{D_2} = 0.0305, \frac{\overline{D_1}}{D_2} = 0.445$$(ratio between mean inlet diameter and outlet diameter), $C_1^* = 0.36$,

$U_1^* = 0.455, C_{2RID}^* = 0.27, \eta_c = 0.58, \eta_G = 0.74$.

It is important to note that having chosen $\beta_{2ID}^? = 90°$ and the triangle of velocity-vectors $C_{2ID}^*, W_{2ID}^*, U_2^* = 1$ turns out to be the one shown in Figure-8.

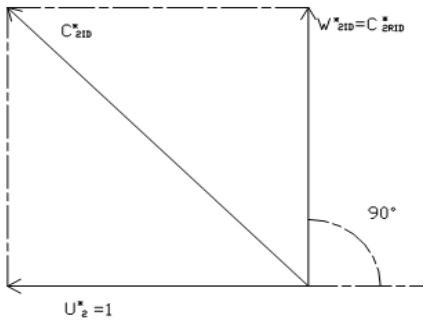

Figure-8. Vector triangle of impeller output velocities.

Design procedure

The design procedure is articulated in the steps summarized in Table-1

Table-1. Design procedure breakdown.

Step #	Input	Output	Equation #
1	Z, β'_{2ID}	slip factor μ	(1)
2	$\mu, W_{2ID}^* = C_{2RID}^*,$	$\overline{C}_2^*, \overline{W}_2^*, U_2^* = 1, \beta_2'$	(2)
3	$W_1^*, \overline{W}_2^*, \beta_2'$	ξ_W (obstruction coefficient of the wake zone)	(4)
4	$\xi_W, \overline{C}_2^*, \overline{W}_2^*, U_2^* = 1$	$C_2^*, W_2^*, U_2^* = 1$	(5)
5	C_{2R}^*, β_2'	Ψ	(13)
6	$\Psi, \eta_C, \frac{P_B^0}{P_A^0}, T_A^0$	U_2	(11)
7	$U_2, C_2^*, W_2^*, U_2^* = 1$	C_2, W_2	
8	$C_2, W_2, U_2, C_1, W_1, U_1$	P_2, T_2, ρ_2	(15)(16)(17)

Given $\rho_2, \dot{m}, \frac{b_2}{D_2}, \xi_2$ the equation (14) can be written in the following way:

$$\dot{m} = \rho_2 \cdot 2\pi r_2 \cdot b_2 \cdot \xi_2 \cdot C_{2R} = \rho_2 \cdot \pi D_2 \cdot D_2 \cdot \frac{b_2}{D_2} \cdot \xi_2 \cdot C_{2R} = \rho_2 \cdot \pi \cdot D_2^2 \cdot \frac{b_2}{D_2} \cdot \xi_2 \cdot C_{2R} \quad (18)$$

from (18) it is possible to evaluate D_2 (19):

$$D_2 = \sqrt{\frac{\dot{m}}{\rho_2 \cdot \pi \cdot \frac{b_2}{D_2} \cdot \xi_2 \cdot C_{2R}}} \quad (19)$$

Given D_2 and $\frac{\overline{D_1}}{D_2}$ (input data) it is possible to calculate $\overline{D_1}$. Given $\overline{D_1}, \rho_1, C_1$, it is possible to evaluate D_{1e}, D_{1i} (20)(21):

$$D_{1e} = \sqrt{\overline{D}_1^2 + \frac{2\dot{m}}{\pi\rho_1 C_1}} \quad (20)$$

$$D_{1i} = \sqrt{\overline{D}_1^2 - \frac{2\dot{m}}{\pi\rho_1 C_1}} \quad (21)$$

Verifying the performance of the impeller

As indicated in the preceding paragraph, the design of the impeller is based on the "a priori" imposition of a few design variables. A particularly critical one is the efficiency of the rotor. It is then necessary to verify that this value is compatible with the results. To perform this verification, we use the method proposed by Osnaghi [3] (14)(15)(16):

$$\eta_G = \frac{\left(\frac{W_{1e}}{U_2}\right)^2 + 1 - \left(\frac{D_{1e}}{D_2}\right)^2 - \frac{1}{\psi^2}\left(\frac{W_2}{U_2}\right)^2}{\left(\frac{W_{1e}}{U_2}\right)^2 + 1 - \left(\frac{D_{1e}}{D_2}\right)^2 - \left(\frac{W_2}{U_2}\right)^2} \quad (22)$$

$$\psi^* = 0{,}012 + 1{,}55\left(\frac{W_2}{W_{1e}}\right) - 0{,}55\left(\frac{W_2}{W_{1e}}\right)^2 + 6{,}07153\,10^{-15}\left(\frac{W_2}{W_{1e}}\right)^3 \quad (23)$$

$$\frac{\psi}{\psi^*} = 1{,}688944 - 1{,}97(M_{aR1e}) + 1{,}945(M_{aR1e})^2 - 0{,}6945(M_{aR1e})^3 \quad (24)$$

RESULTS

The results of the GA optimization are the following: $Z = 18$, $\xi_2 = 0.955$, $\eta_G = 0.74$, $\eta_C = 0.59$, $D_2 = 70$ mm, $b_2 = 2$ mm, $\overline{D}_1 = 31$ mm, $D_{1e} = 41$ mm, $D_{1i} = 17$ mm, $\omega =$ 166,904 rpm

Figure-9. 3D CAD of the impeller.

The final aspect of the impeller is depicted in Figure-9. As can be seen the flux leaving the impeller is supersonic: this result is not surprising when you consider the very high compression ratio required, however it is not unusual for centrifugal compressors. It is therefore necessary to use a vaneless diffuser in which the supersonic flow exiting the impeller is slowed to subsonic speeds. By the way the authors had very poor experiences with vaned diffuser , with poor off-design performance. At this point the design should be validated with CFD (Computational Fluid Dynamic) simulation. This method proved to be quite accurate in performance prediction of centrifugal compressors and it is widely used by the authors when the maps of commercial compressors are not available.

CONCLUSIONS

A GA optimized preliminary design of an extremely high ratio compressor impeller has been described in details. This initial step is strictly necessary to obtain a preliminary design to be furtherly optimized and validated through CFD. A compression ratio of 8:1 was obtained with a very small air flow (500 kg/h) typical of a DID with 150-200 HP output power. The problem of dimensioning of small high ratio compressor is particularly critical, since their design is more difficult than a large turbocharger unit. An efficiency of 58% was obtained. This figure seem to be very small, however given this compression ratio, the lower limit design value was only 45%. In fact a turbocharger with this compression ratio reduces masses and piping, allowing a more reliable power system.

REFERENCES

[1] SANDROLINI S., NALDI G., Le turbomacchine motrici e operatrici, Pitagora.

[2] Yahya. 1983. Turbines, Compressors and Fans, TATA McGRAW-HILL.

[3] OSNAGHI C. 1982. Macchine fluidodinamiche, CLUP.

[4] L. Piancastelli., L. Frizziero., S. Marcoppido., E. Pezzuti. 2012. Methodology to evaluate aircraft piston engine durability. edizioni ETS. International journal of heat & technology. ISSN 0392-8764, Vol. 30, No.1, pages 89-92.

[5] L. Piancastelli., L. Frizziero., G. Zanuccoli., N.E. Daidzic. and I. Rocchi. 2013. A comparison between CFRP and 2195-FSW for aircraft structural designs. International Journal of Heat and Technology. Volume 31, Issue 1, Pages 17-24.

[6] L. Piancastelli., L. Frizziero., N.E. Daidzic. and I. Rocchi. 2013. Analysis of automotive diesel conversions with KERS for future aerospace applications. International Journal of Heat and Technology. Volume 31, Issue 1, pages 143-154.

[7] L. Piancastelli, L. Frizziero, I. Rocchi, 2012. An innovative method to speed up the finite element analysis of critical engine components, International

Journal of Heat and Technology. vol. 30, Issue 2, pp. 127-132.

[8] L. Piancastelli., L. Frizziero. and I. Rocchi. 2012. Feasible optimum design of a turbocompound Diesel Brayton cycle for diesel-turbo-fan aircraft propulsion. International Journal of Heat and Technology. Volume 30, Issue 2, Pages 121-1262.

[9] L. Piancastelli., L. Frizziero., S. Marcoppido., A. Donnarumma. and E. Pezzuti. 2011. Fuzzy control system for recovering direction after spinning. International Journal of Heat and Technology. Volume 29, Issue 2, Pages 87-93.

[10] L. Piancastelli., L. Frizziero., S. Marcoppido., A. Donnarumma. and E. Pezzuti. 2011. Active antiskid system for handling improvement in motorbikes controlled by fuzzy logic. International Journal of Heat and Technology. Volume 29, Issue 2, Pages 95-101.

[11] L. Piancastelli., L. Frizziero., E. Morganti. and E. Pezzuti. 2012. Method for evaluating the durability of aircraft piston engines, Walailak Journal of Science and Technology The Walailak Journal of Science and Technology. Institute of Research and Development, Walailak University. ISSN: 1686-3933, Thasala, Nakhon Si Thammarat 80161. Volume 9, n.4, pp. 425-431,Thailand.

[12] L. Piancastelli., L. Frizziero., E. Morganti. and A. Canaparo. 2012. Embodiment of an innovative system design in a sportscar factory. Pushpa Publishing House, Far East Journal of Electronics and Communications, ISSN: 0973-7006. Volume 9, Number 2, pages 69-98, Allahabad, India.

[13] L. Piancastelli., L. Frizziero., E. Morganti. and A. Canaparo. 2012. The Electronic Stability Program controlled by a Fuzzy Algorithm tuned for tyre burst issues. Pushpa Publishing House, Far East Journal of Electronics and Communications, ISSN: 0973-7006. Volume 9, Number 1, pages 49-68, Allahabad, India.

[14] L. Piancastelli., L. Frizziero., I. Rocchi. and G. Zanuccoli. N.E. Daidzic. 2013. The "C-triplex" approach to design of CFRP transport-category airplane structures. International Journal of Heat and Technology, ISSN 0392-8764. Volume 31, Issue 2, Pages 51-59.

[15] L. Frizziero, I. Rocchi: 2013. New finite element analysis approach. Pushpa Publishing House, Far East Journal of Electronics and Communications, ISSN: 0973-7006, Volume 11, Issue 2, pages 85-100, Allahabad, India.

[16] L. Piancastelli, L. Frizziero, E. Pezzuti 2014. Aircraft diesel engines controlled by fuzzy logic. Asian Research Publishing Network (ARPN), Journal of Engineering and Applied Sciences, ISSN 1819-6608. Volume 9, Issue 1, pp. 30-34, EBSCO Publishing, 10 Estes Street, P.O. Box 682, Ipswich, MA 01938, USA.

[17] L. Piancastelli., L. Frizziero. and E. Pezzuti. 2014. Kers applications to aerospace diesel propulsion. Asian Research Publishing Network (ARPN), Journal of Engineering and Applied Sciences, ISSN 1819-6608. Volume 9, Issue 5, pp. 807-818, EBSCO Publishing, 10 Estes Street, P.O. Box 682, Ipswich, MA 01938, USA.

[18] L. Piancastelli., L. Frizziero. and G. Donnici. 2014. A highly constrained geometric problem: The inside-outhuman-based approach for the automotive vehicles design. Asian Research Publishing Network (ARPN), Journal of Engineering and Applied Sciences, ISSN 1819-6608, Volume 9, Issue 6, pp. 901-906, EBSCO Publishing, 10 Estes Street, P.O. Box 682, Ipswich, MA 01938, USA.

[19] L. Frizziero. and F. R. Curbastro. 2014. Innovative methodologies in mechanical design: QFD vs TRIZ to develop an innovative pressure control system. Asian Research Publishing Network (ARPN), Journal of Engineering and Applied Sciences, ISSN 1819-6608, Volume 9, Issue 6, pp. 966-970, EBSCO Publishing, 10 Estes Street, P.O. Box 682, Ipswich, MA 01938, USA.

[20] L. Piancastelli. and L. Frizziero. 2014. How to adopt innovative design in a sportscar factory. Asian Research Publishing Network (ARPN), Journal of Engineering and Applied Sciences, ISSN 1819-6608. Volume 9, Issue 6, pp. 859-870, EBSCO Publishing, 10 Estes Street, P.O. Box 682, Ipswich, MA 01938, USA.

[21] L. Piancastelli., L. Frizziero. and I. Rocchi. 2014. A low-cost, mass-producible, wheeled wind turbine for easy production of renewableenergy. Published by Pushpa Publishing House, Far East Journal of Electronics and Communications, ISSN: 0973-7006. Volume 12, Issue 1, pages 19-37, Allahabad, India.

[22] L. Piancastelli., G. Caligiana., Frizziero Leonardo. and S. Marcoppido. 2011. Piston engine cooling: an evergreen problem, 3rd CEAS Air&Space Conference – 21st AIDAA Congress – Venice (Italy), 24th-28th October.

[23] L. Piancastelli., L. Frizziero., E. Morganti. and A. Canaparo. 2012. Fuzzy control system for aircraft diesel engines, edizioni ETS, International journal of

heat & technology, ISSN 0392-8764. Vol. 30, N.1, pages 131-135.

Symbols

Symbol	Description	Unit	Value
C1	Impeller inlet absolute velocity	m/s	
C2	Impleller outlet absolute velocity	m/s	
W1	Impeller inlet relative velocity	m/s	
W2	Impleller outlet relative velocity	m/s	
U1	Impeller inlet tangential velocity	m/s	
U2	Impleller outlet tangential velocity	m/s	
C2id,U2id,W2id	Impeller outlet ideal velocities	m/s	
pedix R	Radial component of vector referred to the impeller	m/s	
pedix T	Tangential component of vector referred to the impeller	m/s	
overline	True value	-	
beta	Angle between W and the tangential direction T	-	
ì	Slip factor (Traupel)	-	
Z	Impeller vane number	-	
β_{2ID}	Angle between vane outlet and T	-	
ξ_W	Coefficient of obstruction due to the WAKE area	-	
$\dot{m} =$	Mass flow		
A	Area of the fluid passage	m^2	
ñ	Density of the fluid in the passage area	kg/ m^3	
V	Fluid velocity (component orthogonal to the passage)	m/s	
A_{PID}	Area of passage of the fluid of the impeller without vanes	m^2	
ξ	Vane obstruction coefficient of A impeller	-	
A_P	Area of passage of the fluid of the impeller without vanes	m^2	
k	Adiabatic gas constant	--	
R	Iideal gas constant	J/(kg K)	
T_1^0	Inlet temperature	K	
çc	Compressor efficiency	-	0.58
ø	Work coefficient	-	
P_1^0	Compressor inlet pressure	Pa	
P_2^0	Compressor outlet pressure	Pa	
L	Specific work of the “ideal” adiabatic transformation	J/kg	
b	Thickness of air passage	m	
η_G	Impeller efficency	--	0.74
$M_{aR1e} =$	Mach number at the impeller entrance (e stands for entrance)	--	
ω	IImpeller angular velocity	rpm	